Since January 2020 Elsevier has created a COVID-19 resource centre with free information in English and Mandarin on the novel coronavirus COVID-19. The COVID-19 resource centre is hosted on Elsevier Connect, the company's public news and information website.

Elsevier hereby grants permission to make all its COVID-19-related research that is available on the COVID-19 resource centre - including this research content - immediately available in PubMed Central and other publicly funded repositories, such as the WHO COVID database with rights for unrestricted research re-use and analyses in any form or by any means with acknowledgement of the original source. These permissions are granted for free by Elsevier for as long as the COVID-19 resource centre remains active.

Available online at www.sciencedirect.com
ScienceDirect
Virology 360 (2007) 150–158
VIROLOGY
www.elsevier.com/locate/yviro

Derivation of a novel SARS–coronavirus replicon cell line and its application for anti-SARS drug screening

Feng Ge [a,*], Yonghu Luo [b], Pei Xiong Liew [c], Eugene Hung [a]

[a] *Department of Microbiology, Yong Loo Lin School of Medicine, National University of Singapore, Block MD4, 5 Science Drive 2 Singapore 117597, Republic of Singapore*
[b] *Guangdong Institute of Microbiology, 100 Xianlie Central Road, Guangzhou, Guangdong, 510070, PR China*
[c] *Department of Haematology, Singapore General Hospital, Singapore Health Research Facilities, 7 Hospital Drive, Block A, #02-05, Singapore 169611, Republic of Singapore*

Received 9 August 2006; returned to author for revision 30 August 2006; accepted 1 October 2006
Available online 13 November 2006

Abstract

The severe acute respiratory syndrome (SARS) outbreak in 2002, which had a high morbidity rate and caused worldwide alarm, remains untreated today even though SARS was eventually isolated and controlled. Development and high-throughput screening of efficacious drugs is therefore critical. However, currently there remains a lack of such a safe system. Here, the generation and characterization of the first selectable, SARS–coronavirus (SARS–CoV)-based replicon cell line which can be used for screening is described. Partial SARS–CoV cDNAs and antibiotic resistance/reporter gene DNA were generated and assembled in vitro to produce the replicon transcription template, which was then transcribed in vitro to generate the replicon RNA. The latter was introduced into a mammalian cell line and the transfected cells were selected for by antibiotic application. For the antibiotic-resistant cell lines thus generated, the expression of reporter gene was ensured by continued monitoring using fluorescent microscopy and flow cytometry. The suitability of this replicon cell line in drug screening was demonstrated by testing the inhibitory effect of several existing drugs and the results demonstrate that the SARS–CoV replicon cell lines provide a safe tool for the identification of SARS–CoV replicase inhibitors. The replicon cell lines thus developed can be applied to high-throughput screening for anti-SARS drugs without the need to grow infectious SARS–CoV.
© 2006 Elsevier Inc. All rights reserved.

Keywords: SARS; Coronavirus; SARS–CoV; Reverse genetics; Replicon; Drug screening

Introduction

Severe acute respiratory syndrome (SARS) is a potentially fatal atypical pneumonia that arose in Guangdong Province of the People's Republic of China in November 2002, quickly spreading to 26 countries on five different continents and causing large-scale outbreaks in Hong Kong, Singapore and Toronto in early 2003 (Peiris et al., 2003b). SARS was recognized in late 2002 and by the end of the viral outbreak in July 2003, there have been more than 8000 SARS cases reported worldwide and 774 SARS-attributed deaths (Kuiken et al., 2003). This outbreak had a severe and profound impact on public health and economies worldwide, reminding us of the danger emerging infectious diseases bring to densely populated societies.

Coronaviruses (order *Nidovirales*, family *Coronaviridae*, genus *Coronavirus*) are a group of viruses with large, enveloped crown-like virions and positive-sense single-stranded RNA genomes (Siddell et al., 1983). The genomes of coronaviruses range from 27 to 32 kb, the largest of any of the known RNA viruses. All coronaviruses share the characteristic 3′ co-terminal and nested-set structure of sub-genomic RNAs in addition to unique RNA synthesis strategies, genome organization, nucleotide sequence homology and structural proteins particular only to coronaviruses (Cavanagh et al., 1995).

The etiologic agent of SARS was identified as a novel coronavirus (SARS–CoV) (Peiris et al., 2003a; Drosten et al.,

* Corresponding author. Present address: Department of Clinical Research, SingHealth Research Facilities, Singapore General Hospital, Singapore 169611, Republic of Singapore. Fax: +65 6321 3606.
E-mail address: ge.feng@singhealth.com.sg (F. Ge).

0042-6822/$ - see front matter © 2006 Elsevier Inc. All rights reserved.
doi:10.1016/j.virol.2006.10.016

2003; Ksiazek et al., 2003; Poutanen et al., 2003) although the genomic sequence of SARS–CoV does not resemble any of the three recognized groups of coronaviruses. Soon after the disease was recognized, SARS–CoV was confirmed as the causative agent of SARS; by demonstrating that the coronavirus could be used to experimentally infect and induce interstitial pneumonitis in *Cynomolgus macaques*, thus fulfilling Koch's postulates (Fouchier et al., 2003; Kuiken et al., 2003).

Although the 2002/2003 SARS epidemic was eventually controlled by patient isolation, there is neither an effective treatment for SARS presently nor an efficacious vaccine to prevent infection (Peiris et al., 2003b). The significant morbidity and mortality, including its potential for reemergence, make it necessary to develop effective methods to treat and prevent the disease. Therefore, in the fight against SARS, it is important to develop antiviral agents that can specifically inhibit the RNA synthesis of SARS–CoV.

To maximize the chance of finding efficacious anti-SARS drugs, high-throughput screening of large chemical libraries for compounds that can block SARS–CoV replication must be carried out. However, the high infectivity and virulence of SARS–CoV render this kind of research very dangerous. Therefore, there is a need for an anti-viral agent identification system that does not involve the use of live virus.

To this aim, partial viral RNA genomes have been constructed such that they replicate and persist in dividing cells without producing viral particles (Kaplan and Racaniello, 1988; Liljestrom and Garoff, 1991; Khromykh and Westaway, 1997; Behrens et al., 1998; Lohmann et al., 1999; Pang et al., 2001; Shi et al., 2002; Thumfart and Meyers, 2002; Hertzig et al., 2004). These viral replicons were derived from viral genomes through the deletion of all or some structural genes. Due to the absence of viral structural genes, virion proteins are not synthesized in the cells and therefore no infectious viral particle could be produced by the cells. However, since all *trans*- and *cis*-acting components required for viral RNA synthesis are retained, these partial viral RNAs could replicate autonomously in the cells.

This report describes the construction of the first SARS–CoV-derived replicon cell line. This SARS-associated replicon cell line is based on the use of SARS replicon cDNAs generated by reverse genetic techniques. The results demonstrate that these SARS–CoV-derived replicon cell lines can be used to test candidate SARS–CoV replicase inhibitors without the need to grow infectious SARS–CoV.

Results

Generation of SARS–CoV replicon RNA

Our method of developing replicon constructs was based on the strategy previously used to assemble the full-length cDNA construct SARS–CoV (Yount et al., 2003). The strategy for the construction of the replicon is illustrated in Fig. 1. Viral envelope-protein coding genes *S*, *E* and *M* were excluded from the replicon to disable virion synthesis, production and secretion. The nucleocapsid gene, *N*, was retained because the nucleocapsid protein has been shown to be required for viral RNA synthesis (Almazan et al., 2004; Hertzig et al., 2004) and that the sequence involved in the regulation of the expression of a coronavirus 3′-proximal gene is more than ~50 nt upstream of the gene (Alonso et al., 2002; Jeong et al., 1996). Therefore, to achieve relatively native expression of *N* gene from the replicon, a region ~60 nt upstream of N ORF was included in the replicon. The green fluorescent protein–blasticidin deaminase fusion (*GFP–BlaR*) gene was also included into the replicon to enable easy selection and detection of replicon-containing cells. *GFP–BlaR* gene was inserted between ORF 1 and N, not at the 5′ or 3′ end of the replicon, in order to minimize any possible deleterious effect in the synthesis of replicon RNA. The expression of *GFP–BlaR* was driven by the transcription regulatory sequence of ORF S, which was included in the replicon and occurring at a position right upstream of the *GFP–BlaR* gene. Following this strategy, six cDNA subclones that span the SARS–CoV genome were used in the assembly of recombinant SARS–CoV replicon cDNA. The green fluorescent protein–blasticidin deaminase fusion (*Gb*) gene was amplified from the plasmid pTracer™-CMV/Bsd/LacZ using PCR and included into the replicon constructs. In addition, the cDNAs constructed were flanked by restriction sites that leave unique interconnecting junctions of 3 or 4 nts in length (*Sap*I or *Bsa*I). As these sticky ends are not complementary to the majority of other sticky ends, which are generated by the same enzyme at other sites in the DNA, replicon cDNAs can be systematically assembled by in vitro ligation.

The total DNA from the above ligation reaction, after an extraction using phenol–chloroform, was used directly as the template for the in vitro transcription and synthesis of the SARS–CoV replicon RNA. For a rough quality inspection, an aliquot of the post-transcription mixture was analyzed on a denaturing agarose gel and the transcripts seen were of the appropriate lengths (data not shown).

Generation and analysis of SARS–CoV replicon-carrying cells

The purified SARS–CoV replicon RNA was used to transfect BHK-21 cells and the transfected cells were subjected to blasticidin selection to enrich for the replicon-carrying cells. As fluorescence indicates successful transfection and selection of SARS–CoV replicon RNA, transfected cells were observed for fluorescence microscopically after 5 days of blasticidin treatment. Clusters of green-fluorescent cells were observed and a typical green-fluorescent cell cluster is shown in Fig. 2A. As observed, there was no sign of any cytotoxicity due to the SARS–CoV replicon and the morphology of the green-fluorescent cells was typical of BHK-21 cells. The transfected cultures were further maintained under blasticidin selection to obtain cells that carried the SARS–CoV replicon consistently.

Autonomous replication of viral RNA was also successfully maintained, Northern blot analysis of total cellular RNAs prepared from SCR-1 revealed the presence of full-length replicon RNA and replicon RNA derived transcripts encoding *Gb* and *N* genes. The N gene probe detected replicon RNA

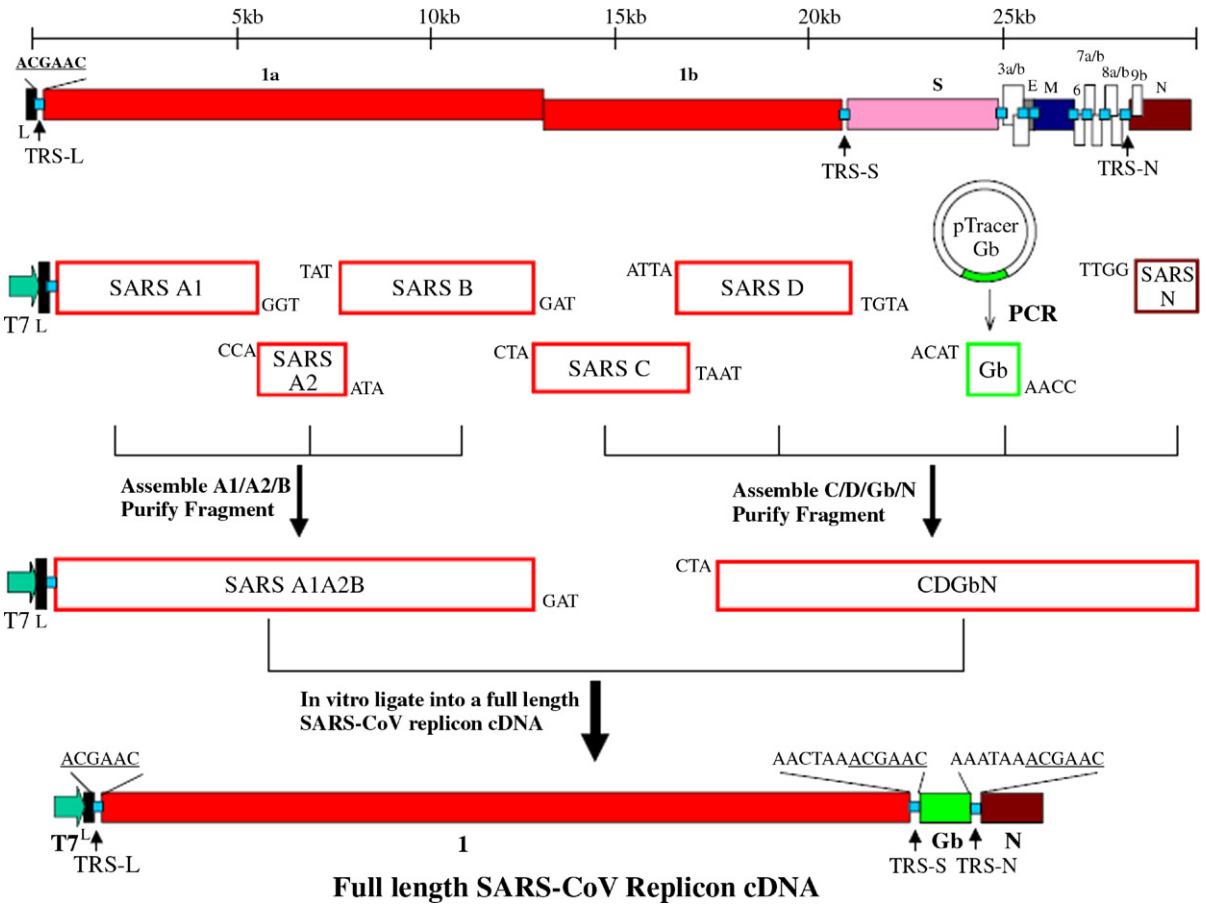

Fig. 1. SARS–CoV replicon and the strategy for its construction. The structural relationship of the SARS–CoV genome and SARS–CoV replicon cDNA is shown. Blue box represents SARS–CoV transcription regulatory sequences (TRSs) site. The 5′-caps and 3′-polyadenine tails of the SARS–CoV genome and replicon RNAs are omitted. *Gb*, green fluorescent protein–blasticidin deaminase fusion gene; L, leader sequence; *S*, spike gene; *N*, nucleocapsid gene; T7, T7 promoter.

and replicon RNA-derived Gb-N and N RNAs. The Gb probe detected only those RNAs containing the *Gb* gene; replicon RNA and replicon RNA-derived Gb-N mRNA (Fig. 2B).

GFP expression of SCR-1 has been studied by fluorescence microscopy and flow cytometry for a period of 3 months (over 40 passages under blasticidin selection). As shown in Fig. 2C, the average green fluorescence intensity value of SRC-1 culture remained at a constant level and was in excess of that of the parent BHK-21 culture. These results were consistent when compared to previous findings (Hertzig et al., 2004). Hertzig et al. (2004) analyzed the GFP expression of HCoV 229E replicon cells by flow cytometry for a period of 4 months (over 50 passages under G418 selection) and they showed that the percentage of green fluorescent cells remained at a constant level of 40–60% throughout this period. Thus, these data indicate that although replicon cells may express sufficient *GFP–BlaR* to survive blasticidin selection, the amount of GFP BlaR protein was insufficient to be detected by flow cytometry. A possible cause for differential GFP BlaR protein expression in replicon cells is the efficiency of functional replicon RNA uptake during transfection. Thus, this analysis shows that the SARS–CoV replicon persists efficiently and grows consistently in the cells under selection for substantial periods of time and would be suitable to use for anti-SARS drug screening purposes. Furthermore, SCR-1 cells that have been stored for 1 month in liquid nitrogen and re-cultured still displayed green fluorescence indistinguishable from cells that have been passaged continuously (data not shown). Subsequent passage of cell culture supernatants onto BHK-21 cells also did not result in either blasticidin resistance or GFP expression, thus demonstrating that the replicon particles are not released by passaging supernatants into fresh cultures.

Sequence analysis of the replicon RNA purified from SCR-1 cells soon after selection in blasticidin (passage number【p】6) found no sequence differences compared with the published sequence of SARS–CoV strain SIN2774 (GenBank Accession Number AY283798). At passage number【p】40, the RNA from SCR-1 cells was purified and examined again by sequence analysis. At this later passage, three nucleotide changes were detected that resulted in three amino acids changes: two in ORF 1 and one in *N* gene (Table 1). Since these nucleotide changes were not encoded by the cloned cDNA and no adaptive mutations had occurred in the early passage, these three mutations, most likely, have been acquired during replication in the later passage. It remains important to elucidate whether the mutations facilitate efficient replication of replicon RNA in SCR-1.

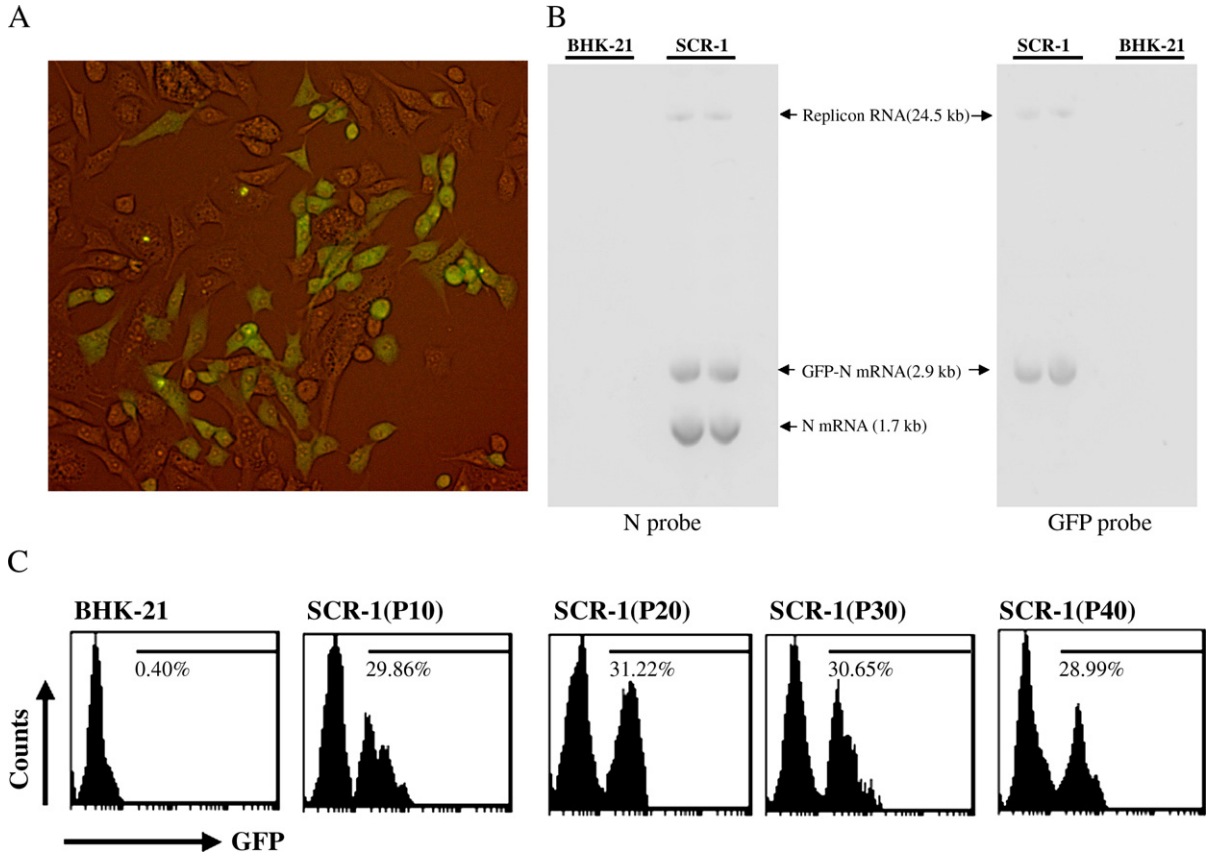

Fig. 2. Analysis of replicon RNA-containing cells. (A) Combined green fluorescence and phase-contrast microscopic images of SCR-1 cells are shown. (B) Presence of SARS–CoV replicon and sub-replicon RNAs in replicon-carrying cells as detected by Northern blot analysis. Total RNA preparations from BHK-21 (BHK) and SCR-1 cells were analyzed as indicated. Arrows indicate full-length replicon RNA and replicon RNA-derived transcripts encoding GFP and N. (C) A flow cytometry analysis of SCR-1 cells is shown. Samples of SCR-1 cells were analyzed at passage number P10, P20, P30 and P40 under blasticidin selection and the parent BHK-21 (BHK) cells were co-analyzed. Indicated values represent the percentages of green fluorescent cells. The results are presented as histograms with green fluorescence intensity in exponential scale (horizontal axis) against cell number in linear scale (vertical axis).

Inhibition of SARS–CoV replication

To develop a fast and convenient antiviral screening protocol for the detection of SARS–CoV replicase inhibitors, three previously described antiviral drugs were tested, all of which have been evaluated in the context of SARS–CoV inhibition in tissue culture (Yount et al., 2003; Cinatl et al., 2003; So et al., 2003). The compounds were applied in different concentrations on SCR-1 cells and GFP expression was monitored by flow cytometry analysis, fluorescent microscopy and quantitative real-time PCR 3 days later. Untreated cells served as controls and the cytotoxic effect of each compound was assessed in parallel on parental BHK-21 cells. As shown in Fig. 3, incubation of SCR-1 cells with E64-d at 0.4 mg/ml reduced not only the level of reporter gene expression and the copy number of replicon RNA but also the overall percentage of green fluorescent cells. Importantly, no cytotoxicity of E64-d was observed at or near inhibitory concentrations. Ribavirin showed low inhibitory activity at the concentration of 0.4 mg/mL and significant cytotoxic effects were observed at higher concentration, 0.5–5 mg/mL. As such, Ribavirin was considered to be inactive against SARS–CoV replication. Glycyrrhizin showed low inhibitory effect at the concentration of 2 mg/mL. These results indicate that the cysteine proteinase inhibitor E64-d appears to represent a promising candidate for the inhibition of SARS–CoV replicase function. On the other hand, the therapeutic efficacy of the other drugs may be limited because of their low specific inhibitory effect and significant cytotoxicity. Taken together, these results show that the replicon cell lines thus developed would be useful for anti-SARS drug screening and will provide a tool to study candidate anti-SARS agents.

Table 1
Sequence analysis of replicon RNA from P40 SCR-1 cells

Encoded domain	Genomic position of nucleotide (SARS–CoV SIN2774)	Nucleotide change (P40 SCR-1)	Amino acid change (P40 SCR-1)
Replicase nsp3	7860	T → C	Tyr → His
Replicase nsp6	11,422	T → C	Val → Ala
Nucleocapsid	28,252	C → T	Thr → Ile

Discussion

In the past 15 years, the concept of autonomously replicating RNAs (replicon RNAs) has been applied to a number of positive-strand RNA virus systems and has led to the establishment of

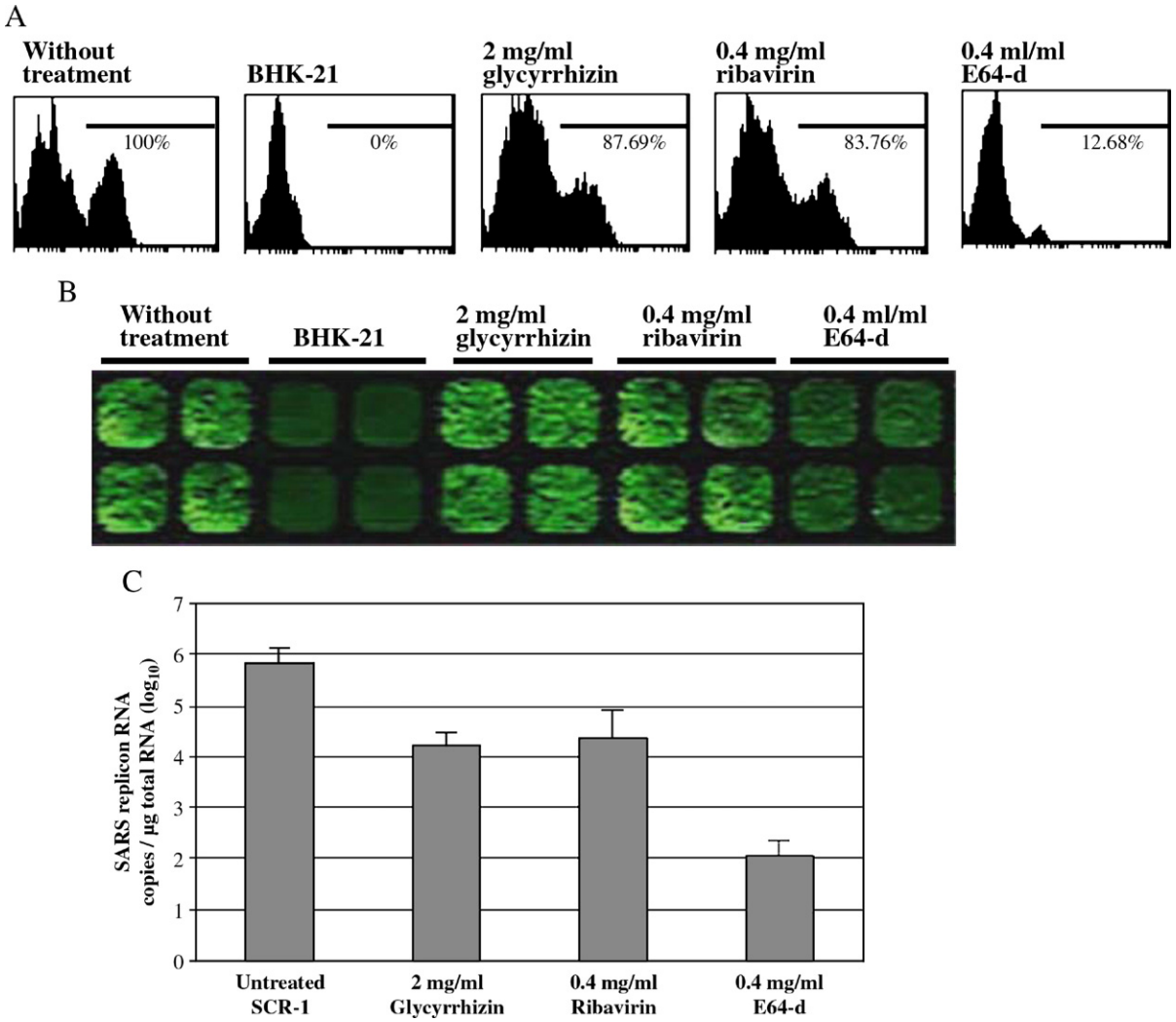

Fig. 3. Inhibition of SARS–CoV replication. SCR-1 cells containing SARS–CoV-based replicon RNA that mediates GFP expression were used to assess the inhibitory effect of the compounds by (A) flow cytometry analysis. One representative experiment out of four is shown. Bars indicate GFP-expressing cells in flow cytometry analyses. The GFP expression of untreated cells was set at 100%. (B) Fluorescence microscopy analysis. Quadruple wells of untreated and treated SCR-1 cells are shown. The parent BHK-21 (BHK) cells were co-analyzed. (C) Quantitative real-time RT–PCR. Copy number of SARS replicon RNA in SCR-1 cells before and after inhibitor treatments are shown. The inhibitors used are indicated below. Data are the means of three independent experiments. Bar: 95% confidence intervals.

novel antiviral screening assays and vectors (Bartenschlager, 2002; Lo et al., 2003). Baric's group constructed a transmissible gastroenteritis virus (TGEV) replicon for the expression of heterologous *GFP* gene (Curtis et al., 2002) and Thiel's group generated a non-cytopathic, selectable replicon RNA (based on HCoV 229E) for the identification of coronavirus replicase inhibitors (Hertzig et al., 2004). Nevertheless, the genomic sequence data of SARS–CoV reveal that this novel agent did not belong to any of the known groups of coronaviruses, including two human coronaviruses, HcoV OC43 and HcoV 229E (Peiris et al., 2003a; Drosten et al., 2003). Therefore, despite the presence of functional replicon RNA assays (Hertzig et al., 2004), there is a need for the development of SARS–CoV replicon cell lines, which would allow a rapid and safe identification of inhibitors that are specific for SARS–CoV.

In this study, the first selectable SARS–CoV based replicon cell line was successfully established and characterized for the purpose of screening anti-SARS drugs. The SARS–CoV replicon cell line we described here will be a valuable tool for the development of anti-SARS therapeutics.

Our results with the following replicase inhibitors clearly demonstrate that our SARS–CoV replicon system facilitates the identification of these inhibitors in tissue culture. Replicase inhibitor Ribavirin, although active against a wide range of viruses and used as SARS therapy (So et al., 2003), was shown in this study to be inactive against SARS–CoV in vitro at non-cytotoxic concentration, which is in line with previous reports (Tan et al., 2004; Cinatl et al., 2003;Wu et al., 2004). Next, the finding that E64-d inhibitor had selective activity against SARS–CoV is in line with a study by Yount et al. (2003), who showed that E64-d effectively inhibited SARS–CoV replication in tissue culture. For glycyrrhizin, the variation in results obtained in this study as compared to previously published results may be due to assay conditions including virus strain,

detection method and compound concentration and handling (Cinatl et al., 2003). Notably, other independent groups also observed the lack of anti-SARS–CoV activity of glycyrrhizin (Hertzig et al., 2004). This indicates that glycyrrhizin may not inhibit coronavirus replication but instead exert antiviral effects during virus adsorption or release.

With an easily detectable GFP expression and the absence of virion production, our viral replicon cell line represents a simpler and safer system for anti-viral agent identification than a live virus infection system. Thus, the efficacy of candidate inhibitors can be evaluated by measuring the fluorescence intensity of the replicon cells before and after the addition of drugs. That means our cell-based system can be easily automated and used in large-scale screening of anti-SARS–CoV agents. Furthermore, our viral replicon cell-based system can be used to test individual antiviral agents designed based on certain biochemical principles or new drugs targeting at multiple regions of the SARS–CoV ORF 1 or *N* gene. Since no infectious virus is formed, the assay represents a safe protocol that can be performed in biosafety level 2 laboratories.

Compared to anti-viral agent identification systems based on purified proteins or nucleic acids, our SARS–CoV replicon cell line has two advantages: first, if a candidate inhibitor can inhibit replication of our replicon RNA, which occurs intracellularly, it thus demonstrates that this agent can permeate the cell. Secondly, the cytotoxicity of the candidate inhibitor can also be observed simultaneously by noting its cell morphology. Two critical indexes of a candidate inhibitor–its inhibitory effect and cytotoxicity, can therefore be met using our SARS–CoV replicon cell line. For an anti-viral agent identified using a purified-bimolecular-based system, further tests on cell delivery and cytotoxicity of the agent has to be done separately.

A disadvantage of our replicon cell-based system is that the structural genes *S*, *E* and *M* are not included in the replicon RNA. Therefore, it cannot be used to screen for drugs that act on cellular and viral targets involved in receptor binding, virus entry, genome encapsulation and virus release. However, structural genes of coronaviruses change rapidly and anti-viral agents that target these genes have less consistent efficacy. Thus, anti-viral agents should target regions highly conserved in the coronavirus genome such as ORF 1, which is the most conserved region found.

In conclusion, our replicon system provides a convenient and safe screening system for the identification of drug candidates selectively active against SARS–CoV. The protocols and reagents developed in this study will be useful for gaining insights into the mechanisms of RNA synthesis of this pathogen. Potential additional applications include the development of RNA vaccines against SARS–CoV and RNA vectors for long-term gene expression.

Materials and methods

Cells and viruses

The baby hamster kidney (BHK)-21 cell line was purchased from American Typical Culture Center (ATCC). BHK-21 cell line was maintained in DMEM medium (Gibco) supplemented with 10% foetal calf serum (Gibco) (D10). SARS–CoV strain SIN2774 virion RNA (a gift of Prof. T. K. Chow, Department of Microbiology, National University of Singapore) was used as the template for cDNA synthesis.

Systematic assembly of SARS–CoV replicon DNA

The reverse genetic strategy for constructing the desired SARS–CoV replicon is illustrated in Fig. 1. The reverse transcription reaction was performed using the SuperScript III First Strand Kit (Invitrogen) as described in the manufacturer's manual with some modifications (Nathan et al., 1995). The reverse transcription was primed using oligonucleotide 9R (5′-GTCATTCTCCTA AGAAGCTATTAAAATCACATGG-3′) and 09R (5′-GATTCAGGTCTC ATTGTCCTCCAC TTGC TAGGTAATCC-3′). The cDNAs were denatured for 30 s at 94 °C and amplified by PCR with Elongase Amplification System (Invitrogen) with 35 cycles at 94 °C for 30 s, 55 °C for 30 s, and 68 °C for 1.5 to 6 min depending on the size of the amplicon. The amplicons were isolated from agarose gels and cloned into Topo II TA vectors (Invitrogen) according to the manufacturer's directions. The following primers were used in the isolation of the SARS A1 subclone (froward, 5′-CACGCTCTTCAGCATAC TAATACGACTCACTATA-GATATTAGGTTTTTACCTACCCAGGAAAAG-3′, reverse, 5′-GAATGAGCTCTTCATGGTAATGGTTGAGTTGG-TACAAGG-3′); A2 subclone (forward, 5′-GAATGAGCT-CTTCACCAAATGCGAGTTTTGATAATTTCB-3′, reverse, 5′-CAACCATCCATGATATGAACATAGC-3′); B subclone (froward, 5′-CCGTTTCTGCAA TGGTTAGGATG-3′, reverse, 5′-GGCTGCTGTAGTCAATGGTATGATG-3′); C subclone (froward, 5′-GCAGATCAGGCTATGACCCAAATGTAC-3′, reverse, 5′-TGGGAGGCTT ATGTGACTTGC-3′); D subclone (froward, 5′-GTGCCTGTATTAGGAGACCATTCC-3′, reverse, 5′-GTATCAGGTCTCAATGTTCGTTTAGTTGT-TAACAAGAATATCAC-3′) and N subclone (froward, 5′-CATTCAGGTCTCATTGGTACCTTCATGAAGGTCACC-3′, reverse, 5′-GTCATTCTCCTAAGAAGCTATTAAAATCA-CATGG-3′). The Gb DNA was amplified as described above, except that the template was pTracer™-CMV/Bsd/LacZ vector DNA (1 ng) and the primers were forward, 5′-CGTGGATC-CGGTCTCTACATGGCCTCCA AAGGAGAAGAAC-3′ and reverse, 5′-CCAGAATTCGGTCTCACCAATTAGCCCTC-CCA CACATAACCAG-3′.

Two to five independent clones of each SARS amplicon were isolated and sequenced using a panel of primers located about 0.5 kb from each other on the SARS insert and an ABI model automated sequencer. The sequencing data thus obtained were compared with the published sequence of SARS–CoV strain SIN2774 (GenBank Accession Number AY283798) using the MegAlign module of the sequence analysis software Lasergene (DNASTAR). A consensus sequence for each of the cloned fragments were determined, and when necessary (i.e., A1, B and D subclones), a consensus clone was assembled using restriction enzymes and standard recombinant DNA techniques to remove unwanted amino acid changes except silent mutations.

Each of the plasmids was grown to high concentration, isolated and digested or double-digested with *Sap*I or *Bsa*I according to the manufacturer's direction (NEB). The appropriately sized cDNA inserts were isolated from 0.7 ~ 1.2% agarose gels and extracted using the Qiaex II DNA purification kit (Qiagen). The A1+A2+B, C+D, and Gb+N fragments were ligated overnight and isolated. The A1A2B+CD+GbN cDNAs were ligated overnight at 4 °C. The resulting DNA was extracted first by phenol–chloroform–isoamyl alcohol (25:24:1), then by chloroform, and precipitated in the presence of 67% ethanol and 0.1 M sodium acetate (pH 5.2). Shortly before the performance of in vitro transcription (see below), the extracted DNA was pelleted by centrifugation, washed with 70% ethanol, air-dried and finally dissolved in 10 μl of RNase-free water. The detailed cloning strategy, plasmid maps and sequences are available from the author upon request.

In vitro transcription, transfection and generation of a stable cell line containing SARS–CoV replicon RNA

The T7 in vitro transcription system mMessage mMachine Kit (Ambion), which also includes the RNA 5′-capping function, was used to generate the SARS–CoV replicon RNA. For 2 h at 37 °C, a 30-μl reaction mix were performed with 4.5 μl of a 30 mM GTP stock, resulting in a 1:1 ratio of GTP to cap analog. To remove the DNA template, 1 μl of DNase I (2 U/μl) was then added and the reaction mix was incubated at 37 °C for 15 min. To polyadenylate the RNA synthesized, the reaction mixture was treated further by the reagents from the Poly (A) Tailing Kit (Ambion). The final product was purified by adding 30 μl of LiCl precipitation solution (Ambion) to pellet the RNA. The RNA was washed once with 1 ml of 70% ethanol, air-dried, and finally dissolved in 20 μl of RNase-free water.

BHK-21 cells grown to 50% confluence in a 6-well plate were transfected with 10 μg of SARS–CoV replicon RNA and 10 μl of the transfection agent Lipofectamine 2000 (Invitrogen) in Opti-MEM medium (Invitrogen) according to the manufacturer's instructions. One day after transfection, blasticidin (Invitrogen) was added to a final concentration of 10 μg/ml to the culture medium to select for the replicon-carrying cells. Two weeks later individual cell clones were isolated and expanded until analysis or storage in liquid nitrogen.

Analysis of SARS–CoV replicon-carrying BHK-21 cell line

The blasticidin-resistant cell line generated was designated as SCR-1 and subjected to analyses pertinent to the SARS–CoV replicon that they carried. The parent cell line BHK-21 was used as the negative control in these analyses.

Fluorescence microscopy and flow cytometry were used to observe the green fluorescence of GFP BlaR protein expressed from the SARS–CoV replicon. The cells were observed under an Olympus IX70 inverted fluorescence microscope and the images were recorded using Image-Pro Plus (Media Cybernetics). The cells were then scanned for green fluorescence and light scattering using a Beckman Coulter Epics Altra flow cytometer. The data collected were analyzed using the WINMDI 2.7 data analysis program (The Scripps Research Institute).

To analyze whether the introduced replicon RNA can mediate coronavirus-specific discontinuous transcription of L-Gb-N and L-N mRNAs (Fig. 4), Northern blot analysis was performed. For Northern blot analysis, total cellular RNAs from BHK-21 or SCR-1 cells were isolated using the RNeasy Mini Kit (QIAGEN) according to the Animal Cell Protocol supplied by the manufacturer. Samples (10 μg) of total cellular RNAs were denatured, electroporated and transferred to a Hybond-N^+ positively charged nylon membrane (Ambion) as per the manufacturer's instructions and hybridized with fluorescein-labelled probes specific for the *Gb* gene or the SARS *N* gene. The Gb and N probes were prepared from the *Gb* and *N* gene using the Gene Images Random Prime Labeling Module (Amersham). The hybridization of probes to the immobilized RNAs on the nylon membrane and subsequent signal generation were done using the reagents from the Gene Images CDP-Star Detection Module (Amersham). Chemiluminescent signals

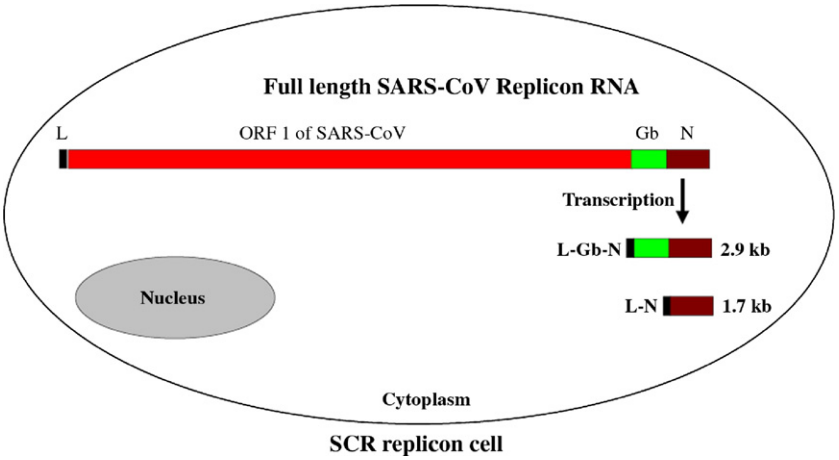

Fig. 4. Generation of sub-replicon RNAs through discontinuous transcription of SARS–CoV replicon RNA in the replicon-carrying cells. The black box represents the 72-nt leader RNA sequence, derived from the 5′ end of the replicon, located at the 5′ end of each sub-replicon RNA. The size of each RNA shown is exclusive of the poly-A tail.

emitted from the blot were detected by exposing a Hyperfilm-MP X-ray film (Amersham) to the blot for durations between 1 to 10 min, followed by the photographic development of the exposed film.

To obtain the complete sequence of the SARS–CoV replicon persisting in the SCR-1 cells, the total cellular RNAs isolated from SRC-1 cells at passage number【P】6 and【P】40 were used as the templates. The RNA was amplified by RT–PCR and the PCR products were gel-purified and sequenced directly. Primers used in the RT–PCR and sequence analysis are available upon request.

To prove that the replicon particles are not released by passaging supernatants into fresh cultures, supernatants obtained from SCR-1 cell cultures were passaged onto fresh BHK-21 cells and examined for blasticidin resistance and GFP expression.

Inhibition of SARS–CoV replication

To identify potential agents active against SARS–CoV replication, three drugs approved for clinical use in the treatment of viral infections were tested. E64-d and glycyrrhizin (Sigma) were included in this test due to their previously reported activities against SARS–CoV replication (Yount et al., 2003; Cinatl et al., 2003). Ribavirin (ICN Pharma) was also used as it represents a widely used class of nucleoside analogs, which inhibits viral polymerases (So et al., 2003). SCR-1 cells were cultured in a 96-well plate in DMEM containing 10% FBS and 10 μg/mL blasticidin. The culture media was removed after a 1-day incubation when the cells reached 80–90% confluence and replaced by fresh medium without blasticidin. Graded doses of drugs were added on monolayers of SCR-1 cells and an untreated well was served as control. Three days later, the cells were harvested and analyzed by fluorescence microscopy and flow cytometry. Four duplicate tests were performed. Inhibition of reporter gene expression was calculated as reduction of the fluorescence intensity of GFP-positive cells by setting the fluorescence intensity of untreated SRC-1 cells at 100%. In parallel, the cytotoxicity of drugs was assayed on BHK-21 cells using CellTiter 96 Aqueous Non-radioactive Cell Proliferation Assay Kits (Promega).

Real-time RT–PCR analyses were performed to quantify the copy number of replicon RNA in SCR-1 cells before and after drug treatment. Total cellular RNAs from BHK-21 or SCR-1 cells were isolated using the RNeasy Mini Kit and One-step Artus SARS LC RT–PCR kit (QIAGEN, Hamburg, Germany) was used for real-time quantitative amplification of SARS–CoV replicon RNA. Real time RT–PCRs were performed according to the instructions of the manufacturer. The amplicon and primers were as described (Drosten et al., 2003). Briefly, 5 μl of total RNA extract was added to a capillary tube containing 15 μl of RT–PCR reagents and loaded into the LightCycler (Roche Diagnostics GmbH, Mannheim, Germany). The thermal cycling conditions were as follows: RT was performed at 50 °C for 10 min; and amplification was performed for 1 cycle of 95 °C for 10 s, followed by 50 cycles of 2 s of denaturing at 95 °C, 12 s of annealing at 55 °C, and 10 s of extension at 72 °C. Finally, cooling was performed at 40 °C for 30 s. Total RNA extracted from BHK-21 cells was used as the negative control. Internal SARS–CoV standards, which allow the determination of the copy number of replicon RNA, were supplied with the assay kit. Real-time PCR signals were analyzed using the LightCycler software (Roche; version 5.32), and the sizes and uniqueness of PCR products were verified by performing both melting curves and agarose gel electrophoresis. The copy number of replicon RNA was determined by direct comparison with the internal standards. Replicon RNA expression levels are expressed as number of copies/μg total RNA. All samples were run in triplicate and the average value of the copy number was employed to quantify replicon RNA.

Acknowledgments

Ge Feng gratefully acknowledges the continuous support by Dr. Zhang Xian-en over many years. We thank Dr. Yu Hongxiang and Professor Mary Ng for their excellent assistance, and the Roche company that provided compounds for the assay experiment. This study was funded by a grant from the Biomedical Research Council, Singapore.

References

Almazan, F., Galan, C., Enjuanes, L., 2004. The nucleoprotein is required for efficient coronavirus genome replication. J. Virol. 78, 12683–12688.

Alonso, S., Izeta, A., Sola, I., Enjuanes, L., 2002. Transcription regulatory sequences and mRNA expression levels in the coronavirus transmissible gastroenteritis virus. J. Virol. 76, 1293–1308.

Bartenschlager, R., 2002. Hepatitis C virus replicons: potential role for drug development. Nat. Rev., Drug Discov. 1, 911–916.

Behrens, S.E., Grassmann, C.W., Thiel, H.J., Meyers, G., Tautz, N., 1998. Characterization of an autonomous subgenomic pestivirus RNA replicon. J. Virol. 72, 2364–2372.

Cavanagh, D., Brian, D.A., Brinton, M.A., 1995. Virus taxonomy. Sixth Report of the International Committee on Taxonomy of Viruses. Springer-Verlag, Vienna, pp. 407–411.

Cinatl, J., Morgenstern, B., Bauer, G., Chandra, P., Rabenau, H., Doerr, H.W., 2003. Glycyrrhizin, an active component of liquorice roots, and replication of SARS-associated coronavirus. Lancet 361, 2045–2046.

Curtis, K.M., Yount, B., Baric, R.S., 2002. Heterologous gene expression from transmissible gastroenteritis virus replicon particles. J. Virol. 76, 1422–1434.

Drosten, C., Gunther, S., Preiser, W., van der, W.S., Brodt, H.R., Becker, S., 2003. Identification of a novel coronavirus in patients with severe acute respiratory syndrome. N. Engl. J. Med. 348, 1967–1976.

Fouchier, R.A., Kuiken, T., Schutten, M., 2003. Aetiology: Koch's postulates fulfilled for SARS virus. Nature 423, 240.

Hertzig, T., Scandella, E., Schelle, B., Ziebuhr, J., Siddell, S.G., Ludewig, B., Thiel, V., 2004. Rapid identification of coronavirus replicase inhibitors using a selectable replicon RNA. J. Gen. Virol. 85, 1717–1725.

Jeong, Y.S., Repass, J.F., Kim, Y.N., Hwang, S.M., Makino, S., 1996. Coronavirus transcription mediated by sequences flanking the transcription consensus sequence. Virology 217, 311–322.

Kaplan, G., Racaniello, V.R., 1988. Construction and characterization of poliovirus subgenomic replicons. J. Virol. 62, 1687–1696.

Khromykh, A.A., Westaway, E.G., 1997. Subgenomic replicons of the flavivirus Kunjin: construction and applications. J. Virol. 71, 1497–1505.

Ksiazek, T.G., Erdman, D., Goldsmith, C.S., 2003. A novel coronavirus associated with severe acute respiratory syndrome. N. Engl. J. Med. 348, 1953–1966.

Kuiken, T., Fouchier, R.A.M., Schutten, M., Rimmelzwaan, G.F., van Amerongen, G., van Riel, D., Laman, J.D., de Jong, T., van Doornum,

G., Lim, W., Ling, A.E., Chan, P.K.S., Tam, J.S., Zambon, M.C., Gopal, R., Drosten, C., van der Werf, S., Escriou, N., Manuguerra, J.C., Stohr, K., Peiris, J.S.M., Osterhaus, A., 2003. Newly discovered coronavirus as the primary cause of severe acute respiratory syndrome. Lancet 362, 263–270.

Liljestrom, P., Garoff, H., 1991. A new generation of animal cell expression vectors based on the Semliki Forest virus replicon. Biotechnology 9, 1356–1361.

Lo, M.K., Tilgner, M., Shi, P.Y., 2003. Potential high-throughput assay for screening inhibitors of West Nile virus replication. J. Virol. 77, 12901–12906.

Lohmann, V., Korner, F., Koch, J., Herian, U., Theilmann, L., Bartenschlager, R., 1999. Replication of subgenomic hepatitis C virus RNAs in a hepatoma cell line. Science 285, 110–113.

Nathan, M., Mertz, L.M., Fox, D.K., 1995. Optimizing long RT–PCR. Focus 17, 78–80.

Pang, X., Zhang, M., Dayton, A.I., 2001. Development of dengue virus type 2 replicons capable of prolonged expression in host cells. BMC Microbiol. 1, 18.

Peiris, J.S.M., Lai, S.T., Poon, L.L.M., 2003a. Coronavirus as a possible cause of severe acute respiratory syndrome. Lancet 361, 1319–1325.

Peiris, J.S.M., Yuen, K.Y., Osterhaus, A.D.M., Stohr, K., 2003b. The severe acute respiratory syndrome. N. Engl. J. Med. 349, 2431–2441.

Poutanen, S.M., Low, D.E., Henry, B., 2003. Identification of severe acute respiratory syndrome in Canada. N. Engl. J. Med. 348, 1995–2005.

Shi, P.Y., Tilgner, M., Lo, M.K., 2002. Construction and characterization of subgenomic replicons of New York strain of West Nile virus. Virology 296, 219–233.

Siddell, S.G., Wege, H., ter Meulen, V., 1983. The biology of coronaviruses. J. Gen. Virol. 64, 761–766.

So, L.K.-Y., Lau, A.C.W., Yam, L.Y.C., Cheung, T.M.T., Poon, E., Yung, R.W.H., Yuen, K.Y., 2003. Development of a standard treatment protocol for severe acute respiratory syndrome. Lancet 361, 1615–1617.

Tan, E.L., Ooi, E.E., Lin, C.Y., Tan, H.C., Ling, A.E., Lim, B., Stanton, L.W., 2004. Inhibition of SARS coronavirus infection in vitro with clinically approved antiviral drugs. Emerg. Infect. Dis. 10, 581–586.

Thumfart, J.O., Meyers, G., 2002. Feline calicivirus: recovery of wild-type and recombinant viruses after transfection of cRNA or cDNA constructs. J. Virol. 76, 6398–6407.

Wu, C.Y., Jan, J.T., Ma, S.H., Kuo, C.J., Juan, H.F., Cheng, Y.S., Hsu, H.H., Huang, H.C., Wu, D., Brik, A., Liang, F.S., Liu, R.S., Fang, J.M., Chen, S.T., Liang, P.H., Wong, C.H., 2004. Small molecules targeting severe acute respiratory syndrome human coronavirus. Proc. Natl. Acad. Sci. U. S. A. 101, 10012–10017.

Yount, B., Curtis, K.M., Fritz, E.A., Hensley, L.E., Jahrling, P.B., Prentice, E., Denison, M.R., Geisbert, T.W., Baric, R.S., 2003. Reverse genetics with a full-length infectious cDNA of severe acute respiratory syndrome coronavirus. Proc. Natl. Acad. Sci. U. S. A. 100 (22), 12995–13000.